Published online 16 July 2013 *Nucleic Acids Research, 2013, Vol. 41, No. 17* ***8391–8402***
doi:10.1093/nar/gkt621

Dystrophin rescue by *trans*-splicing: a strategy for DMD genotypes not eligible for exon skipping approaches

Stéphanie Lorain[1,*], Cécile Peccate[1], Maëva Le Hir[1,2], Graziella Griffith[1,2], Susanne Philippi[1,2], Guillaume Précigout[1,2], Kamel Mamchaoui[1], Arnaud Jollet[1], Thomas Voit[1] and Luis Garcia[1,2]

[1]Thérapie des maladies du muscle strié, Um76 UPMC - UMR 7215 CNRS - U974 Inserm - Institut de Myologie, 75013 Paris, France and [2]UFR des Sciences de la Santé, Université de Versailles Saint-Quentin-en-Yvelines, 78180 Montigny-le-Bretonneux, France

Received November 27, 2012; Revised June 21, 2013; Accepted June 24, 2013

ABSTRACT

RNA-based therapeutic approaches using splice-switching oligonucleotides have been successfully applied to rescue dystrophin in Duchenne muscular dystrophy (DMD) preclinical models and are currently being evaluated in DMD patients. Although the modular structure of dystrophin protein tolerates internal deletions, many mutations that affect nondispensable domains of the protein require further strategies. Among these, *trans*-splicing technology is particularly attractive, as it allows the replacement of any mutated exon by its normal version as well as introducing missing exons or correcting duplication mutations. We have applied such a strategy *in vitro* by using cotransfection of pre–*trans*-splicing molecule (PTM) constructs along with a reporter minigene containing part of the dystrophin gene harboring the stop-codon mutation found in the *mdx* mouse model of DMD. Optimization of the different functional domains of the PTMs allowed achieving accurate and efficient *trans*-splicing of up to 30% of the transcript encoded by the cotransfected minigene. Optimized parameters included mRNA stabilization, choice of splice site sequence, inclusion of exon splice enhancers and artificial intronic sequence. Intramuscular delivery of adeno-associated virus vectors expressing PTMs allowed detectable levels of dystrophin in *mdx* and *mdx4Cv*, illustrating that a given PTM can be suitable for a variety of mutations.

INTRODUCTION

Splice-switching oligonucleotides acting as steric blockers at the level of the spliceosomal machinery are being developed as treatments for the severe neuromuscular disorder, Duchenne muscular dystrophy (DMD). Two approaches have already proven to be successful in preclinical models. First, synthetic oligonucleotides chemically modified to resist endogenous nucleases, 2′-O-methyl-phosphorothioates and morpholino-phosphorodiamidates, are already under clinical evaluation (1–6). Second, gene therapy has been used to deliver minigenes encoding antisense splice-switching sequences within modified small nuclear RNAs such as U7 or U1 snRNAs (7–15).

DMD represents a suitable test bed for therapeutic exon skipping because the modular structure of the dystrophin protein, and in particular its central rod-domain comprising 24 spectrin-like repeats, tolerates large internal deletions (16). Dystrophin is absent in DMD owing to mutations disrupting the open reading frame. In a milder form of the disease, Becker muscular dystrophy, mutations create shortened but in-frame transcripts that encode a partially functional dystrophin. Exon skipping strategy converts an out-of-frame mutation into an in-frame mutation leading to an internally deleted but partially functional dystrophin. Therefore, depending on the skipped exon(s), the rescued proteins will at best improve dystrophic phenotypes toward milder Becker-like phenotypes. More than 80% of DMD mutations are considered as eligible for this personalized medicine involving the skipping of a single or of multiple exons (17). Nevertheless, this strategy is restricted to patients with genetic diseases for which exon skipping restores a truncated but functional protein and many pathological conditions escape this prerequisite. Unfortunately for the

*To whom correspondence should be addressed. Tel: +33 1 40 77 96 35; Fax: +33 1 53 60 08 02; Email: stephanie.lorain@upmc.fr

others and in particular for patients carrying a mutation in the last third of the DMD gene encoding domains essential to the dystrophin function (10% of DMD population), the exon skipping strategy is not appropriate.

For these reasons, we thought to develop a *trans*-splicing approach that allows the replacement of any mutated exon by its normal version as well as introducing missing exons or correcting duplication mutations. *Trans*-splicing mechanisms were initially observed in lower eukaryotes where mature mRNAs can be produced from two distinct premessengers (18). More recently, a similar mechanism has also been described in mammalian cells and is thought to participate in the molecular diversity of proteins (19). Spliceosome-mediated RNA *trans*-splicing (20) is an mRNA repair strategy based on the splicing in *trans* of two transcripts: the endogenous mutated pre-mRNA and an exogenous engineered RNA, the pre–*trans*-splicing molecule (PTM). The PTM contains the therapeutic sequence to be introduced into the final repaired mRNA, and also contains an antisense domain for annealing specific intronic sequences within the target pre-mRNA, followed by a hemi-intron providing an acceptor splice site recognized by the splicing machinery. *Trans*-splicing has the advantage over conventional gene therapy that it takes place only when and where the target pre-mRNA is expressed, thereby preserving both levels and tissue specificity of the expression of the repaired transcript. Because the coding domain can consist of one or more exons, a single PTM can address diverse mutations spread over several exons. The majority of *trans*-splicing studies have developed therapeutic RNAs replacing the 3′ part of the transcript to be repaired. They have been applied successfully in various contexts of genetic diseases like hemophilia A (21), spinal muscular atrophy (22), X-linked immunodeficiency (23) and cystic fibrosis, in which the widespread mutation CFTRΔF508 was replaced efficiently *in vivo* by the normal sequence via a *trans*-splicing reaction (24). In contrast, only a few attempts for 5′ replacement (25) and for exon replacement by double–*trans*-splicing that we and other recently reported (26,27) have been successful using minigenes.

In the present study, we describe the optimization of PTM constructs designed to repair dystrophin transcripts in the *mdx* mouse. First, we showed a proof of concept for dystrophin transcript repair by cotransfection of a dystrophin minigene and a variety of *trans*-splicing constructs differing in their functional domains. We then demonstrated the feasibility of repairing mutated dystrophin transcripts *in vivo* in two DMD mouse models, *mdx* (nonsense mutation in exon 23) and *mdx4Cv* (nonsense mutation in exon 53), as well as in muscle cells from DMD patients. These results suggest that the *trans*-splicing strategy could be suitable for a wide range of DMD patients for whom exon skipping strategies are not applicable.

MATERIALS AND METHODS

Plasmids

The murine dystrophin minigene target and the plasmid pSMD2-AS2-E23 were already described (26). The E23 lysine codon (nucleotide +196, where nucleotide +1 is the first E23 nucleotide) was transformed from AAA to AAG, creating a HindIII restriction site. For pSMD2-E23-E59/E70, pSMD2-E23-E59/E70opt and pSMD2-E23-E59/E79opt, E59/70, E59/70opt and E59/79opt inserts were obtained by polymerase chain reaction (PCR) on normal dystrophin and optΔR4-R23 (28) complementary DNAs (cDNAs) with the respective primer pairs, E23-E59-F and E70-R, E23-E59opt-F and E70opt-R and E23-E59-F and E79-R (see Supplementary Table S1 for primer sequences), and inserted in pSMD2-AS2-E23 construct in HindIII/EcoR1 restriction sites. 3′SSB and 3′SSC synthetic oligonucleotides were introduced by PCR in pSMD2-E23-E59/E70opt to replace 3′SSA. The artificial intron (133 bp), composed of the 5′ donor splice site from the first intron of the human β-globin gene and the branch point and 3′ acceptor splice site (3′SS) from the intron of an immunoglobulin gene heavy chain variable region, was subcloned by PCR from pCI-neo Mammalian Expression Vector (Promega) into Ale1 blunt restriction site. pSMD2-ΔCMV-AS2-3′SSC-E23-E59/79opt and pSMD2-Δlinker-E23-E59/79opt were created from pSMD2-AS2-3′SSC-E23-E59/79opt by PCR, deleting, respectively, the CMV promoter and the hemi-intron. All expression cassettes subcloned in pSMD2 backbone are under the control of the strong CMV promoter and a polyA signal.

Human dystrophin sequence E59 to E79 STOP codon were amplified from human myotubes cDNA, while antisense sequences (ASs) were amplified from human genomic DNA. Human ASs bind to dystrophin intron 58: AS1 targets nucleotides −445 to −295 and AS2, −145 to +5 (where nucleotide +1 is the first E59 nucleotide). An EcoR1 restriction site was inserted by PCR at nucleotide 81 in E60 (GGC > GGA, both codons encoding glycin). The PTM expressing cassettes were subcloned into pRRL-cPPT-mcs-WPRE plasmid under hPGK promoter (29). All the constructs were verified by sequencing and quantified by spectrophotometer.

Fibroblast transfection

Mouse embryonic fibroblast NIH3T3 cells (ATCC) were maintained in Dulbecco's modified Eagle's medium (DMEM; Life Technologies) supplemented with 10% heat-inactivated FBS (Life Technologies), 100 U/ml penicillin and 100 µg/ml streptomycin. For transfections, cells were grown to 70% confluence in 12-well plates and exposed to the DNA/jetPEI (Polyplus transfection) complex. Typically, 250 ng of dystrophin minigene and 750 ng of PTM plasmids were used in each transfection. The plasmids used in cotransfection experiments with pSMD2-dystrophin minigene (10 215 bp) are as follows: pSMD2 (6206 bp), pSMD2-AS2-E23 (6257 bp), pSMD2-AS2-E23-E59/70 (7492 bp), pSMD2-AS2-E23-E59/70opt or pSMD2-AS2-3′SSA-E23-E59/70opt (7492 bp), pSMD2-AS2-3′SSB-E23-E59/70opt (7519 bp), pSMD2-AS2-3′SSC-E23-E59/70opt (7507 bp), pSMD2-AS2-3′SSA-E23-E59/70opt-Intron (7625 bp).

Recombinant adeno-associated virus vector production and animal experiments

Adeno-associated virus (AAV)2/1 vectors were generated using a three-plasmid transfection protocol as described (30). All animal procedures were performed according to an institution-approved protocol and under appropriate biological containment. Eight-week-old C57BL/6, *mdx* and *mdx4Cv* mice were injected with 50 µl phosphate buffered saline containing 0.4E + 12 AAV genome vectors into the *tibialis anterior*. Four weeks later, mice were sacrificed and muscles collected, snap-frozen in liquid nitrogen-cooled isopentane and stored at −80°C. AAV genomes were detected with primers E23-F and E59optext (primers B/D in Figure 2A) on genomic DNAs extracted from mouse muscles using Puregene Blood kit (Qiagen) as described (31).

Lentiviral production and human myoblast transduction

Lentiviral vectors pseudotyped with the VSV-G protein were produced by transient quadri-transfection into 293T cells and assayed by quantitative real-time PCR on genomic DNA (32). Human myoblasts (33), control CHQ5B and DMD immortalized HSK (34), were grown in the proliferation medium composed of DMEM (Life Technologies) supplemented with 20% fetal calf serum. Myoblasts (1.5E + 04) plated the day before in 12-well plates were transduced with lentivector (3E + 07vg) in 500 µl of proliferation medium and diluted 4 h later by adding 500 µl of proliferation medium. The dishes were incubated for 24 h at 37°C and 5% CO_2 before washing. To induce differentiation, cultures were switched to differentiation medium composed of DMEM with apotransferrin (100 µg/ml, Sigma-Aldrich) and insulin (10 µg/ml, Sigma-Aldrich) and the myotubes were harvested 2 weeks later.

RNA isolation and reverse transcription-PCR analysis

Total RNA was isolated from transfected cells, mouse muscles and human myotubes by using NucleoSpin® RNA II (Macherey-Nagel). Reverse transcription (RT) was performed on 200 ng of RNA by using the Superscript II and random hexamers (Life Technologies). Dystrophin cDNAs from *in vitro* experiments were amplified by PCR with E22-F and E23-R primers (see Supplementary Table S1 for primer sequences) for amplification of total dystrophin transcripts, E22-F and *mdx*E23-R primers for mutated dystrophin transcripts and E22-F and wtE23-R for repaired transcripts (35).

Dystrophin cDNAs from *in vivo* experiments were amplified by nested PCR with E20ext-E26ext external primers and E20int and E26int internal primers for detection of endogenous dystrophin transcripts (primers A/C in Figure 2A) (10); E20ext and E59optext and E22-F and E59optint for *trans*-spliced dystrophin transcripts (primers A′/D); and E23-F and E59optext by single-round PCR for PTMs (primers B/D).

Dystrophin cDNAs from human myotubes transduced with lentivectors expressing PTMs were amplified by nested PCR with hE58ext-hE64ext external primers and hE58int and hE64int internal primers for detection of endogenous dystrophin transcripts (primers E/F in Figure 5B), and E58ext and WPREext and hE58int and WPREint for *trans*-spliced dystrophin transcripts (primers E/H).

RT-PCR products were separated by electrophoresis in 2% agarose gels with ethidium bromide and sequenced.

The number of wild-type dystrophin transcripts as a percentage of total dystrophin transcripts was measured by absolute quantitative real-time RT-PCR method using SsoFast™ EvaGreen® Supermix (Bio-Rad) and E22-F, wtE23-R and E23-R primers. As reference samples, dystrophin cDNA fragments, E22-*mdx*E23-E24 and E22-E23-E24, were cloned into the pCR®2.1-TOPO® and 10-fold serially diluted (from 10^7 to 10^3 copies). Real-time PCR was performed and analyzed on a DNA Engine Opticon 2 (Bio-Rad). All the plasmids were quantified by spectrophotometer.

Immunohistochemistry

A series of 12 µm muscle transverse sections were examined by immunohistochemistry for dystrophin expression using the mouse monoclonal antibody MANEX1B (36). Monoclonal antibodies were detected by Alexa 488 goat anti-mouse antibodies (Life Technologies). Mounted sections were analyzed by confocal laser microscopy (Leica).

RESULTS

Trans-splicing efficiency was dependent on the PTM availability

The classic murine model of dystrophin deficiency, the *mdx* mouse, carries a nonsense mutation in exon 23 of the dystrophin gene (37). To repair the *mdx* dystrophin transcripts, we designed PTM (Figure 1A) containing (i) an antisense sequence (AS) complementary to intron 22, (ii) an hemi-intron including a spacer sequence, a strong conserved yeast branch point sequence (BP), a polypyrimidine tract (PPT) and a canonical 3′SS and (iii) wild-type dystrophin exonic sequence. Based on our recent screen to identify the optimal antisense annealing site within intron 22 (upstream of the mutated exon 23) (26), we selected antisense AS2, of length 150 nt, for efficient dystrophin mRNA repair experiments by *trans*-splicing.

We constructed three PTM plasmids containing different exonic sequences: (i) the murine wild-type E23 alone (AS2-E23), (ii) E23 linked to the E59-70 block of exons (AS2-E23-E59/70) and (iii) E23 followed by E59-70 block of exons optimized for mRNA stability and codon usage while retaining the wild-type protein sequence (AS2-E23-E59/70opt) (28). The first exon (exon 23) of this PTM was not optimized so as not to alter exonic splice enhancers (ESEs), which likely contribute to the *trans*-splicing activity. The latter two PTMs were designed to generate *trans*-spliced transcripts encoding endogenous E1 to E23 in frame with E59 to E70 (Figure 1B). Thus the protein encoded by the *trans*-spliced product would include the same domains as the microdystrophin ΔR4-R23/ΔCT (16),

shown to substantially rescue the *mdx* phenotype (38), but also include spectrin-type repeats R4 through to the first half of R7. To facilitate the analysis of dystrophin premessenger splicing in tissue culture, we used the dystrophin *mdx* gene E22-*mdx*E23-E24 already described (26). Dystrophin minigene and PTM plasmids were cotransfected into the mouse embryonic fibroblast NIH3T3 cell-line, which does not express dystrophin. Total RNA was collected 72 h after transfection and analyzed by RT-PCR with primers designed to detect specifically transcripts resulting from *cis*- and *trans*-splicing events: using a forward primer E22-F specific for E22, and reverse primers specific for either *mdx* E23 (*mdx*E23-R) or wild-type E23 (wtE23-R), respectively, and E23-R for all dystrophin transcripts (Figure 1B). Cells transfected with only the mutation-bearing dystrophin minigene displayed a single 193 bp amplicon with E22-F/*mdx*E23-R primers corresponding to the *cis*-spliced *mdx* dystrophin transcript E22-*mdx*E23-E24 but not with E22-F/wtE23-R primers (Ctrl *mdx* in Figure 1C). Equally, cDNAs from cells transfected only with a plasmid bearing the wild-type murine dystrophin cDNA displayed a 193 bp band with E22-F/wtE23-R primers but not E22-F/*mdx*E23-R (Ctrl wt), confirming the specificity of our assay. In samples that received the *mdx* dystrophin minigene and one of the three PTM plasmids, the wild-type band was detected, signifying that *trans*-splicing events occurred. Absolute quantitative PCR indicated a *trans*-splicing efficacy (number of *trans*-spliced mRNAs as a percentage of total minigene dystrophin mRNAs) of 6.6% ± 1.1 with AS2-E23 (E23) and 8.7% ± 3.3 with the longer PTM AS2-E23-E59/70 (nonoptimized) (Figure 1D). Sequence optimization of the E59/70 region resulted in a considerably greater mRNA repair efficacy of 23% ± 4.2 (optimized). In these experiments, 750 ng of PTM construct were transfected with 250 ng of dystrophin minigene construct, which corresponds to 5-fold more PTM plasmid copies than minigene plasmids for AS2-E23 and 4-fold more for AS2-E23-E59/70 (nonoptimized and optimized). At the mRNA level, a 3-fold ratio was observed for the small transcript AS2-E23 (~470 bases), but was reduced to 0.4- and 0.8-fold for the longer (~2000 bases) PTMs AS2-E23-E59/70 (nonoptimized and optimized, respectively) (Supplementary Figure S1). The greater stability of the optimized over the nonoptimized PTM correlates with the greater observed efficacy noted above (2.6-fold greater: 23 versus 8.7%), suggesting that stabilization of the exonic sequence had an important influence on *trans*-splicing efficacy.

Acceptor splice site strength had no effect on *trans*-splicing efficiency, whereas intron insertion enhanced its efficiency

To design an optimal PTM to rescue dystrophin in the *mdx* mouse model, we assessed three different 3′SSs (Figure 1E) in the pSMD2-AS2-E23-E59/70opt construct. The 3′SSA used in previous experiments corresponded to the 3′ splice site commonly used in published *trans*-splicing studies; 3′SSB consisted of the 39 nucleotides upstream of the second leader exon of the adenovirus major late transcription unit, considered as a particularly strong acceptor splice site (39); and 3′SSC used in recently published *trans*-splicing studies (40). These splice motives presented variable strength when evaluated by maximum entropy scores (MaxEnt): 4.29, 13.01 and 9.44, respectively (Figure 1E), whereas the best MaxEnt score for a 3′ splice site has been estimated to ~14 (41). Surprisingly, although these constructs displayed 3′SS of different strengths, cotransfection experiments with the dystrophin minigene showed similar *trans*-splicing efficiencies (Figure 1F). In contrast, introducing an artificial intron, chosen for its small size compatible with the packaging limit of AAV vectors, into the dystrophin cDNA increased significantly the *trans*-splicing efficiency from 17.8% ± 3.0 to 29.6% ± 4.1.

Dystrophin recovery in *mdx* muscles after delivery of AAV-PTM

AAV1 vectors expressing PTM AS2-3′SSC-E23-E59/79opt were produced and injected into *tibialis anteriors* (TA) of wild-type C57BL/6 (B6) and *mdx* mice. *Trans*-splicing efficiency was evaluated 4 weeks after injection by RT-PCR using a set of PCR primers for specific detection of the different dystrophin transcripts produced in treated muscles (Figure 2A): endogenous transcripts (primers A/C), exogenous dystrophin sequence harbored by PTMs (primers B/D) and *trans*-spliced chimera transcripts (primers A′/D). As expected, the presence of *trans*-spliced transcripts (primers A′/D) was exclusively detected in treated muscles (*mdx* and B6 mice) in which exogenous material from PTM was also identified (primers B/D) (Figure 2B). Direct sequencing of the A′/D amplicon obtained from injected *mdx* muscles confirmed a precise splice junction (endogenous E22–exogenous E23) and the wild-type exon 23 sequence (TAA > CAA) of the *trans*-spliced transcript (Figure 2C). In addition, the amplification of endogenous transcripts with primers (A/C) revealed a single band encompassing exons 20 to 26, confirming that annealing of the PTM to intron 22 of the endogenous dystrophin pre-mRNA did not promote skipping of exon 23. Furthermore, in the absence of CMV promoter driving the PTM expression or of the hemi-intron, no *trans*-spliced transcripts were detected (respectively, ΔCMV and Δlinker, in Figure 2B), therefore excluding hypotheses that chimera PCR amplicons could arise from vector/genome DNA recombination or PCR artifacts. Although high-efficiency transduction procedures were applied (Supplementary Figure S2A), the amount of repaired dystrophin mRNA was only ~1% of total dystrophin transcripts as estimated by semiquantitative RT-PCR (Figure 2D). Accordingly with this low *trans*-splicing efficiency, subsequent levels of microdystrophin were barely detectable by western blot (Supplementary Figure S3), although only few muscle fibers were positively stained by using an antibody recognizing the N-terminal moiety of the dystrophin, which was not encoded by the PTM (Figure 4). These data established the proof of principle of dystrophin mRNA repair by *trans*-splicing in *mdx* muscles.

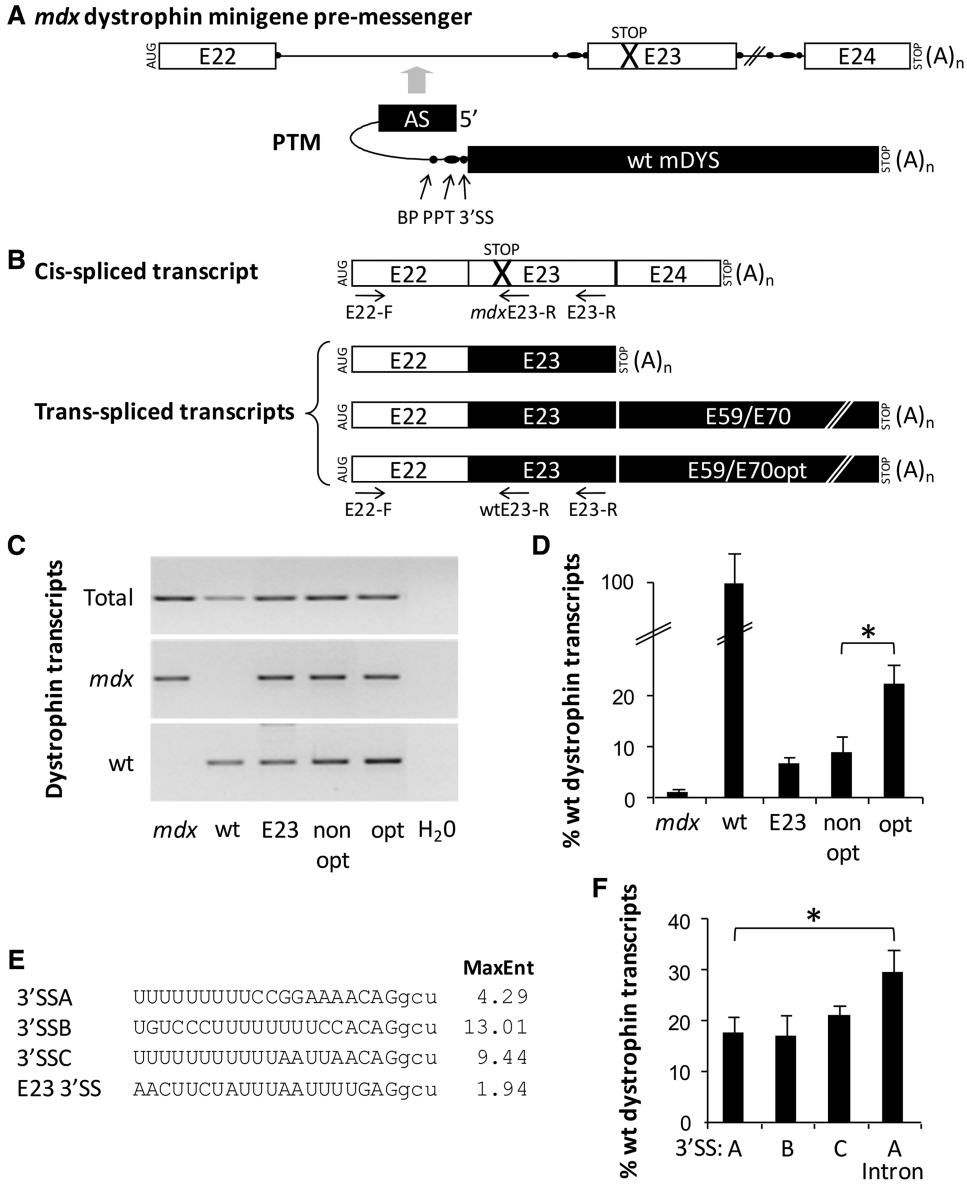

Figure 1. 3′ replacement strategy by *trans*-splicing for dystrophin transcript repair. (**A**) Schematic representation of the dystrophin reporter minigene and PTM. The murine dystrophin premessenger consists of exons (boxes) and introns (lines with black balls illustrating the splice sites). The cross represents the nonsense *mdx* mutation in exon 23 (E23). The PTM is a transcript comprising a 150 nt AS complementary to intron 22 as well as a spacer, a strong conserved yeast BP, PPT, a 3′ acceptor site (3′SS, the three last elements are represented as blacks balls) and part of dystrophin wild-type coding sequence. (**B**) Expected dystrophin transcripts generated by *cis*- and *trans*-splicing. NIH3T3 cells were cotransfected with *mdx* dystrophin minigene and PTM expressing plasmids pSMD2-AS2-E23, pSMD2-AS2-E23-E59/70 and pSMD2-AS2-E23-E59/70opt. Arrows indicate the positions of forward E22-F and reverse E23-R, *mdx*E23-R and wtE23-R PCR primers in the cDNAs produced from those transcripts. (**C**) Detection of repaired dystrophin transcripts by *trans*-splicing. RT-PCR analysis was performed using PCR primers E22-F and E23-R (Total), *mdx*E23-R (*mdx*) and wtE23-R (wt) on NIH3T3 cells cotransfected with dystrophin minigene and pSMD2 (*mdx*), pSMD2-AS2-E23 (E23), pSMD2-AS2-E23-E59/70 (nonoptimized) and pSMD2-AS2-E23-E59/70opt (optimized). 'wt', transfection with the murine wild-type cDNA construct alone. 'H_2O', PCR negative control. Representative results from three independent transfection experiments. (**D**) Quantification of dystrophin mRNA repair by *trans*-splicing. Absolute quantitative RT-PCR was used to evaluate the percentage of wild-type dystrophin transcripts on the total dystrophin transcripts in the experiment presented in (C). The data represent the mean values of three independent transfection experiments ± SD. *$P \leq 0.05$, Student's t-test. (**E**) Sequences of three different 3′ splice sites. Maximum entropy scores (MaxEnt) of the 3′ splice sites A, B and C of the PTMs (3′SSA, B and C) as well as the endogenous E23 3′SS were calculated with an algorithm developed by Burge and colleagues (http://genes.mit.edu/burgelab/maxent/Xmaxentscan_scoreseq_acc.html). (**F**) Quantification of dystrophin mRNA repair. NIH3T3 cells were cotransfected with *mdx* dystrophin minigene and PTM expressing plasmids pSMD2-AS2-3′SSA-E23-E59/70opt (3′SSA), pSMD2-AS2-3′SSB-E23-E59/70opt (3′SSB), pSMD2-AS2-3′SSC-E23-E59/70opt (3′SSC) and pSMD2-AS2-3′SSA-E23-E59/70opt-Intron (3′SSA Intron, pSMD2-AS2-3′SSA-E23-E59/70opt with an artificial intron inserted into the dystrophin cDNA). Absolute quantitative RT-PCR was used to evaluate the percentage of wild-type dystrophin transcripts in the total dystrophin transcripts. The data represent the mean values of three independent transfection experiments ± SD. *$P \leq 0.05$, Student's t-test.

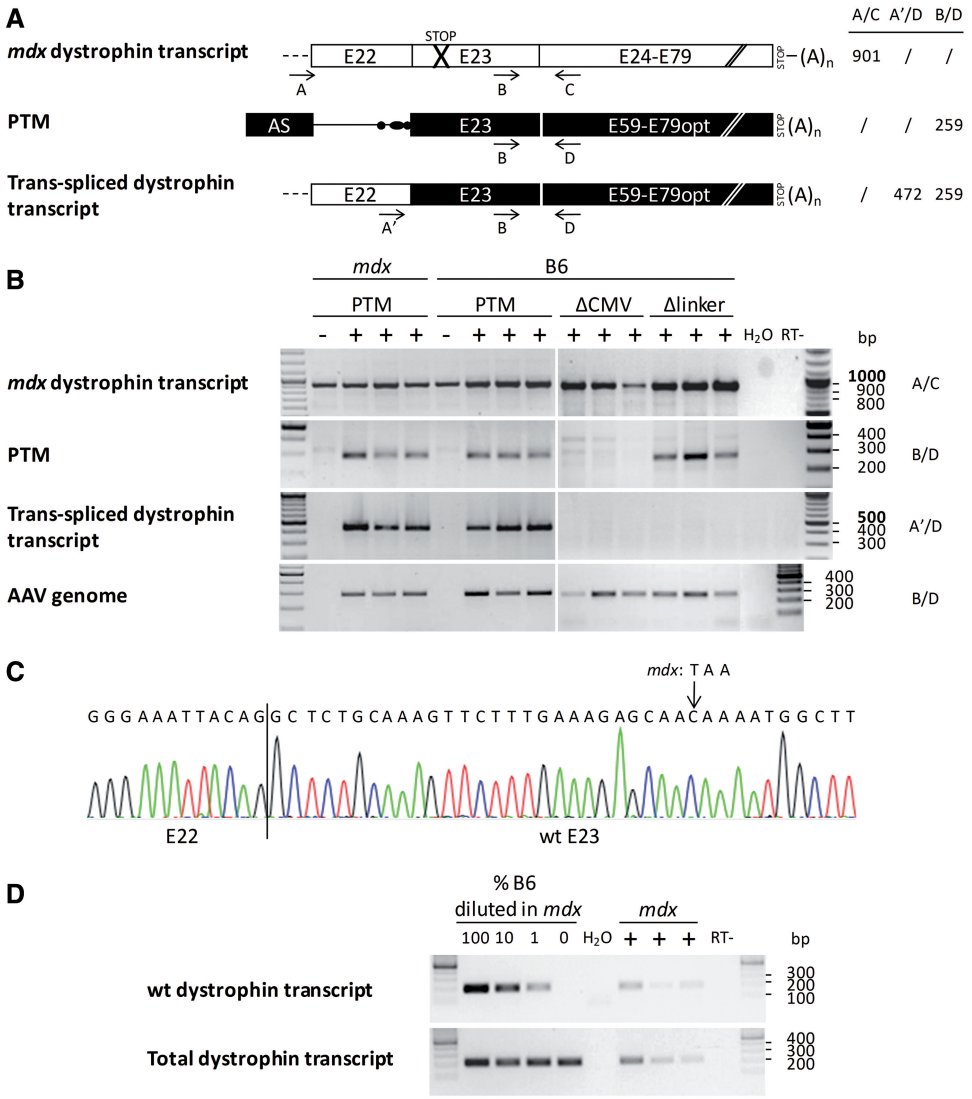

Figure 2. Dystrophin mRNA analysis after intramuscular injection of AAV1 expressing PTMs. (**A**) Expected dystrophin transcripts generated by *cis*- and *trans*-splicing. Arrows indicate E20ext-E26ext external primers and E20int and E26int internal primers used for nested PCR for detection of endogenous dystrophin transcripts (primers A/C) (10); E20ext and E59optext and E22-F and E59optint for *trans*-spliced dystrophin transcripts (primers A′/D); and E23-F and E59optext by single-round PCR for PTMs (primers B/D). The size in bp of expected amplicons is specified. (**B**) Detection of *trans*-spliced dystrophin transcripts *in vivo*. RT-PCR analysis was performed using PCR primers described in A on RNAs extracted from *mdx* and B6 muscles injected (+) or not (−) with AAV1-AS2-3′SSC-E23-E59/79opt (PTM), AAV1-ΔCMV-AS2-3′SSC-E23-E59/79opt (ΔCMV) and AAV1-Δlinker-E23-E59/79opt (Δlinker). AAV genomes were detected with primers B/D on genomic DNAs. 'RT-', PTM injected B6 sample without RT; 'H_2O', PCR negative control. Analysis of three different injected TAs is presented. One of two representative experiments is shown. (**C**) Confirmation of *in vivo trans*-splicing events. An exact E22-E23 junction and wild-type E23 sequence were confirmed by sequencing of the A′/D amplicon obtained from injected *mdx* muscles. (**D**) Determination of the percentage of repaired dystrophin transcripts *in vivo*. Semiquantitative RT-PCR was used to amplify repaired dystrophin transcripts (upper panel) and total dystrophin transcripts (lower panel). Total dystrophin cDNAs were first amplified with E22-F/E23-R3 (15 cycles). The column-purified amplicons were used as matrix for a second PCR round (30 cycles) with E22-F/wtE23-R for repaired dystrophin transcripts (193 bp amplicon) and E22-F/E23-R for total dystrophin transcripts (308 bp amplicon). Band intensities from three PTM injected *mdx* TAs (+) (100 ng of RNAs) were compared with reference wild-type samples in which B6 RNAs were mixed to *mdx* RNAs (100, 10, 1 and 0% of B6 RNAs in 100 ng of total RNAs). 'RT-', PTM injected *mdx* sample without RT; 'H_2O', PCR negative control. Analysis of three different injected TAs is presented. One of two representative experiments is shown.

Dystrophin rescue in *mdx4Cv* muscles

To illustrate that the *trans*-splicing technology is applicable to other mutation patterns, we tested the same PTM in the *mdx4Cv* mouse, which carries a nonsense mutation in exon 53, 30 exons downstream of the classical *mdx* mutation (42). As in the *mdx* mouse, the PTM targeted intron 22 of the *mdx4Cv* dystrophin pre-mRNA to generate *trans*-spliced transcripts encoding endogenous E1 to E23 in frame with E59 to E79 (Figure 3A). AAV1 vectors expressing the PTM AS2-3′SSC-E23-E59/79opt were injected into TA muscles of *mdx4Cv* mice. *Trans*-splicing efficacy was evaluated 4 weeks after injection by RT-PCR using a set of PCR primers for specific detection of the different dystrophin transcripts produced in treated

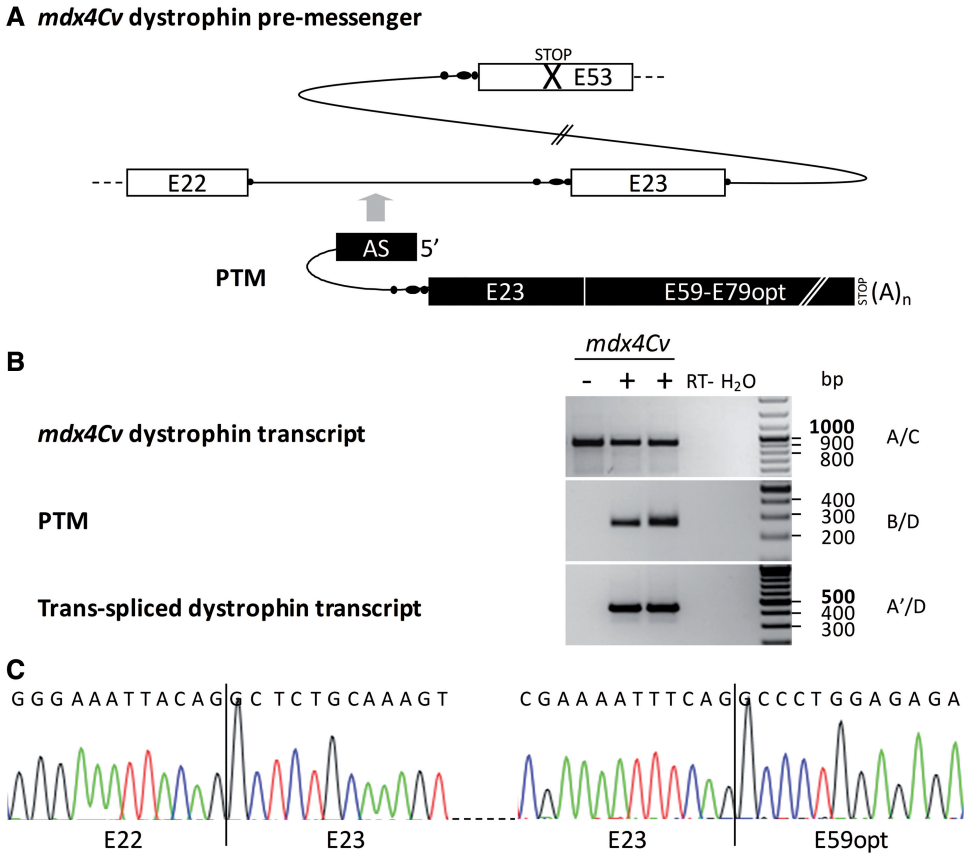

Figure 3. Dystrophin mRNA analysis in *mdx4Cv* muscles after intramuscular injection of AAV1 expressing PTMs. (**A**) 3′ replacement strategy for *mdx4Cv* dystrophin transcript repair. Endogenous *mdx4Cv* dystrophin premessenger is represented with the nonsense mutation in E53 (black cross) as well as the PTM AS2-3′SSC-E23-E59/79opt targeting intron 22. (**B**) Detection of *trans*-spliced dystrophin transcripts *in vivo*. RT-PCR analysis was performed using PCR primers described in Figure 2A on RNAs extracted from *mdx4Cv* TA injected (+) or not (−) with AAV1-AS2-3′SSC-E23-E59/79opt. 'RT-', *mdx4Cv* injected sample without RT; 'H_2O', PCR negative control. Analysis of two different injected TAs is presented. One of two representative experiments is shown. (**C**) Confirmation of *in vivo trans*-splicing events. An exact E22-E23 junction, wild-type E23 sequence and E23-E59opt junction were confirmed by sequencing of the A′/D amplicon obtained from injected *mdx4Cv* muscles.

muscles (Figure 2A): endogenous transcripts (primers A/C), exogenous dystrophin sequence harbored by PTMs (primers B/D) and *trans*-spliced chimera transcripts (primers A′/D). Figure 3B shows dystrophin *trans*-spliced transcripts along with PTMs in injected muscles. Subsequent microdystrophin was correctly localized at the sarcolemma of *mdx4Cv* muscle fibers (Figure 4). Thus, one PTM is compatible with multiple mutations of a given gene.

Dystrophin mRNA rescue in human myotubes

Finally, we tested this *trans*-splicing approach in cells from DMD patients. Two PTM plasmids were designed containing (i) an AS complementary to intron 58; (ii) a hemi-intron including a spacer sequence, a strong conserved yeast BP, a polypyrimidine tract and the 3′SSC; and (iii) the human dystrophin cDNA from E59 to E79 STOP codon (Figure 5A). Two ASs of 150 nucleotides were chosen to match either to the middle of intron 58 (AS1) or to the endogenous 3′SS of intron 58 (AS2). The idea was to test whether getting the PTM close to its target, the 5′ donor splice site of intron 58, or, on the contrary, masking the 3′SS would facilitate *trans*-splicing. An EcoR1 restriction site was created by introducing an isosemantic change at nucleotide 81 in E60 (GGC > GGA, both codons encoding glycin) dystrophin cDNA to discriminate the exogenous sequence. Lentivectors expressing PTMs AS1 and AS2 were produced and used to transduce human wild-type CHQ5B myoblasts and immortalized HSK myoblasts from a DMD patient with a nonsense mutation in exon 71 (TCT > TAA at codon 3420). Myotubes were harvested after differentiation, and total RNA isolated for appraising *trans*-splicing efficiency by RT-PCR using a set of PCR primers for specific detection of the different dystrophin transcripts (Figure 5B): total dystrophin transcripts (primers E/F), and *trans*-spliced chimera transcripts (primers E/H). As expected, the presence of *trans*-spliced transcripts (primers E/H) was exclusively detected in CHQ5B and HSK cells transduced with lentivectors expressing PTMs (AS1 or AS2) (Figure 5C). Direct sequencing of the E/H amplicon obtained from transduced HSK myotubes confirmed a precise splice junction (endogenous E58–exogenous E59), the E60 EcoR1 restriction site and the wild-type E71 of the

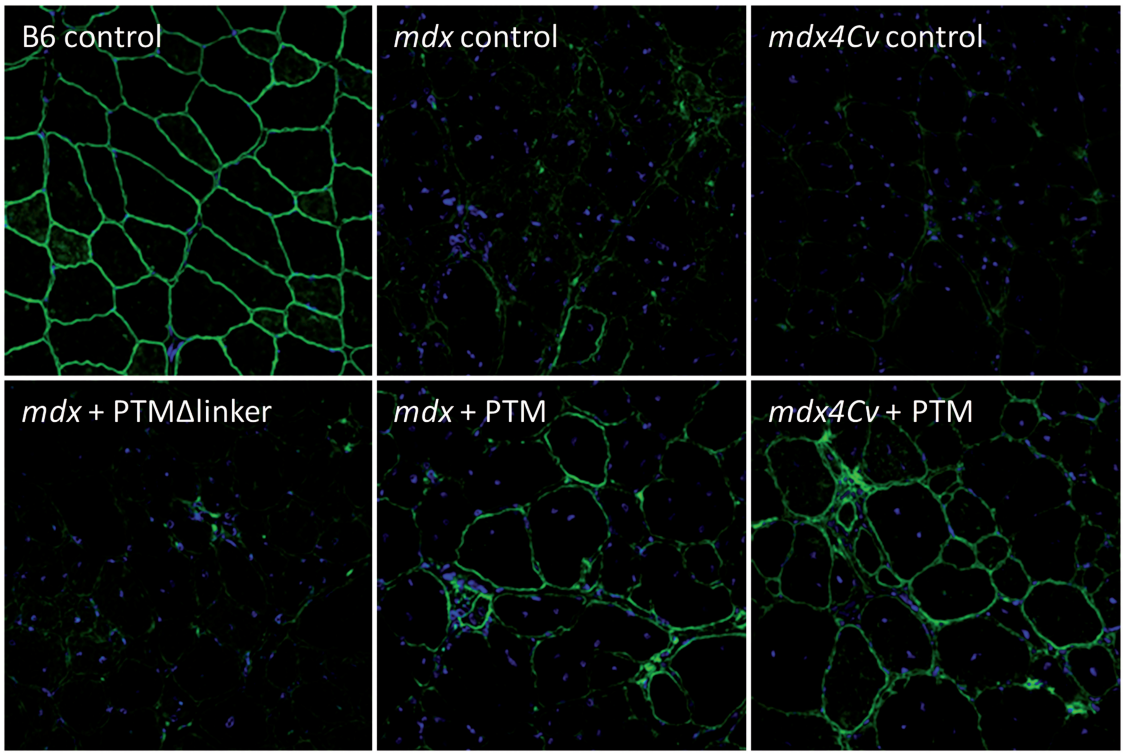

Figure 4. Dystrophin rescue in *mdx* and *mdx4Cv* muscles after intramuscular injection of AAV1 expressing PTMs. Subsarcolemmal localization of the microdystrophin expressed from *trans*-spliced transcripts. Transversal sections from B6, *mdx* and *mdx4Cv* muscles injected or not with AAV1 expressing AS2-3′SSC-E23-pE59/79opt (+PTM) or Δlinker-E23-E59/79opt (+PTMΔlinker) were immunostained with MANEX1B monoclonal antibody recognizing the N-terminal moiety of the dystrophin.

trans-spliced transcript (Figure 5D). Despite efficient lentiviral transduction (Supplementary Figure S2B), no dystrophin protein was detected by western blot.

DISCUSSION

This work shows for the first time the possibility to rescue dystrophin in two murine models of DMD harboring different mutations by using the same *trans*-splicing approach. The design of *trans*-splicing molecules was not straightforward owing to the lack of clear rules for the selection of the different elements constitutive of the PTM molecules. PTMs for 3′ replacement are made of an AS linked to a hemi-intron harboring an acceptor splice site preceding the coding sequence to be *trans*-spliced. However, in the absence of clear guidelines for the selection of these elements, PTM constructs are currently designed and tested empirically. So far, efforts have been focused on determining the best sites for annealing PTMs to target pre-mRNAs. Here, we focused on the consequences of mRNA stabilization by using GeneArt technology, ESE strength, the use of a variety of splice sites and the cooperative effect of internal introns within the PTM.

We speculated that stabilizing the PTM as a single-stranded RNA would result in increased *trans*-splicing efficiency. We used optimized coding sequences of the PTM by GeneArt technology and showed *in vitro* that the number of optimized PTMs was doubled compared with nonoptimized PTMs and subsequent *trans*-splicing efficacy was 2.6-fold greater compared with control. The GeneArt optimization has been shown to considerably increase protein yield thanks to a combination of factors that stabilize mRNA and maximize translational efficacy while retaining the protein sequence, among these are increased GC-content, removal of destabilizing RNA elements, avoidance of RNA secondary structures and codon choice (28). However, the first exon (exon 23) of this PTM was not sequence optimized so as to retain ESEs that likely contribute to the *trans*-splicing activity by defining the acceptor splice site of the PTM molecule. Besides, we thought that these ESEs could be modified to further increase their strength and add force to the *trans*-splicing activity. This was achieved by using the ESEfinder software, which guided the choice of several silent nucleotide changes in ESEs at the level of the exon 23 of the PTM (Supplementary Figure S4A) (43,44). In particular, two nucleotide changes—nucleotide 15 from E23 beginning (UCU > UCC, both codons encoding serine) and nucleotide 16 (UUG > CUG, both codons encoding leucine)—were introduced to increase the score value for SC35 protein binding from 2.7 to 5.2 (E23 ESE1, Supplementary Figure S4B). In parallel, we constructed a PTM with an isosemantic change at nucleotide 57 in exon 23 (E23 ESE2: ACU > ACG, both codons encoding threonine) that increased the score for SRp40 binding from 2.8

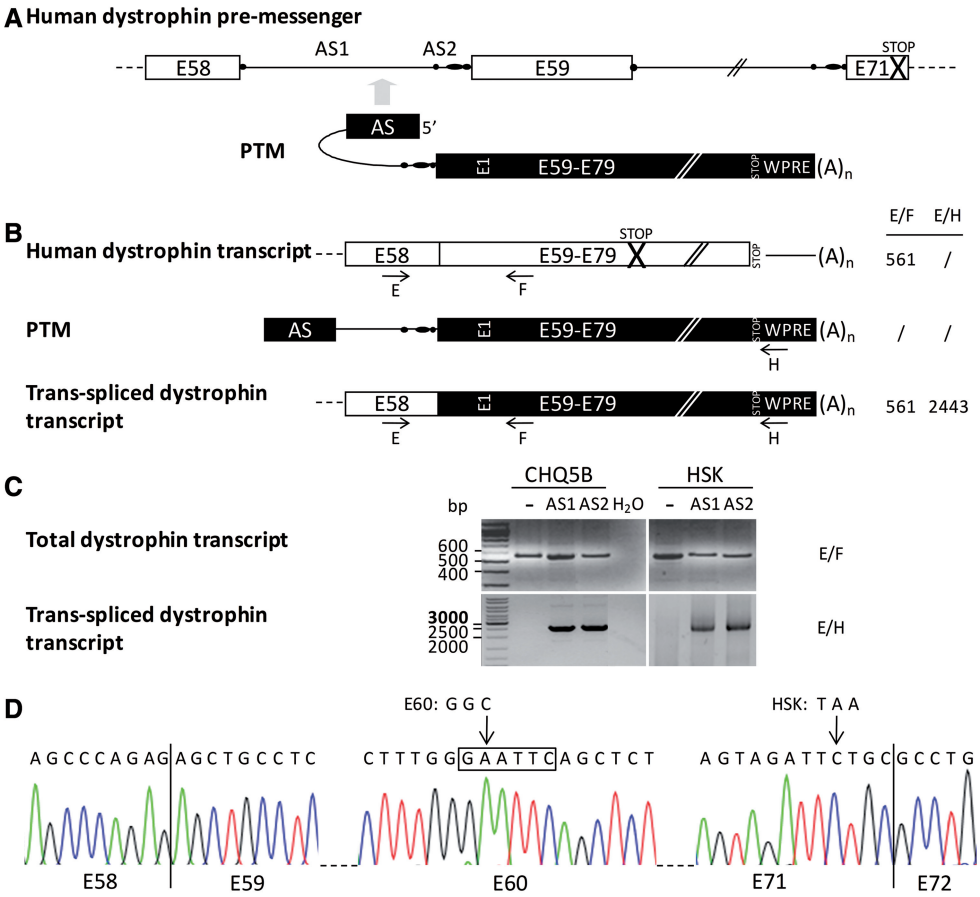

Figure 5. Dystrophin mRNA analysis of human myoblasts transduced with lentivectors expressing PTMs. (**A**) 3′ replacement strategy for human dystrophin transcript repair. The endogenous human dystrophin premessenger is illustrated with E58 and E59 as white boxes and introns as black lines. The cross represents the HSK nonsense mutation in E71. PTMs comprise a 150 nt AS complementary to intron 58 as well as a spacer, a strong conserved yeast BP, a PPT, a 3′SS (the three last elements are represented as blacks balls) and the human dystrophin cDNA from E59 to E79 STOP codon. An EcoR1 restriction site (E1) was introduced in E60. Two PTM constructs were made with different ASs, AS1 and AS2. (**B**) Expected dystrophin transcripts generated by *cis*- and *trans*-splicing. Arrows indicate hE58ext-hE64ext external primers and hE58int and hE64int internal primers used for nested PCR for detection of total dystrophin transcripts (primers E/F), and E58ext and WPREext and hE58int and WPREint for *trans*-spliced dystrophin transcripts (primers E/H). The size in bp of expected amplicons is specified. (**C**) Detection of *trans*-spliced dystrophin transcripts. RT-PCR analysis using PCR primers E/F and E/H on total RNAs extracted from CHQ5B and HSK myotubes transduced or not ('-') with lentivectors expressing PTMs with AS1 and AS2. 'H_2O', PCR negative control. Representative results from two independent transduction experiments. (**D**) Confirmation of *trans*-splicing events in human myotubes. An exact E58-E59 junction, the presence of the EcoR1 restriction site in E60 and wild-type E71 were confirmed by sequencing of the E/H amplicon obtained from transduced HSK myotubes.

to 5.2. Although the new score values for binding SC35 and SRp40 were dramatically higher than threshold values (which are 2.4 and 2.7, respectively), *trans*-splicing efficiencies were not improved (Supplementary Figure S4C).

In theory, to obtain efficient *trans*-splicing, the acceptor splice site of the PTM must be stronger than the endogenous site on the target pre-mRNA with which it competes. Here, the murine exon 23 presents a weak 3′ splice site as illustrated by its extremely low MaxEnt (1.94 in Figure 1E) and suggested experimentally in exon skipping experiments. Indeed, masking the 5′ donor splice site of exon 23 was sufficient to skip this exon from the final transcript (10,45). In addition, another effect of the *mdx* nonsense mutation (C > T transition at nucleotide 28 of exon 23) was to lessen a cluster of ESEs weakening the exon definition even further (46). Based on that knowledge, we thought that we might improve *trans*-splicing efficiency by altering the acceptor splice site of the PTM. However, our *in vitro* tests of several PTMs with variable splice site strength did not impact on the *trans*-splicing efficiency, while levels of those molecules per minigene transcript were not significantly different. This could be explained by the fact that the tested splice sites already have superior strengths than the endogenous one, suggesting that the global context is more important than each functional element considered individually.

Conversely, introducing a foreign intron into the coding sequence of the PTM significantly increased its efficiency. Introns are classically introduced within the 5′ untranslated regions of cDNA transgenes to be highly expressed (47). As already proposed for PTMs (25), such engineering might improve exon definition and therefore facilitate mRNA processing by stimulating localization to the spliceosome where *trans*-splicing reactions can take place (48,49).

It is thought that *trans*-splicing approaches have the advantage over conventional gene therapy to take place only when and where target transcripts are expressed, thus preserving both levels and tissue specificities of the expression of the repaired transcript. In addition, because the coding domain can consist of one or more exons, a given PTM would be able to address diverse mutations spread over several exons. We demonstrated this idea for DMD mutations by *in vivo* experiments in two *mdx* models: the classical one carrying a nonsense mutation in exon 23 and the *mdx4Cv*, which instead carries a nonsense mutation in exon 53. In both cases, *trans*-spliced transcripts were easily detected a few weeks after intramuscular delivery of an AAV vector encoding the PTM. However, the interpretation of these results must be moderated when discussed in the context of therapeutic outcome. Indeed, *trans*-splicing technology is still challenged by efficiency issues. Although functional restoration might reach at best 20% in paradigms such as CFTR rescue (50), repair mRNA levels are always modest (~1%). In our case, although we obtained *in vitro* 30% of minigene transcripts repaired by *trans*-splicing, only 1% of total dystrophin transcripts were repaired *in vivo*. Although some muscle fibers were positive for dystrophin staining, such low levels of dystrophin were yet not detectable by using western blot techniques, advising that *trans*-splicing approaches demand further optimization to achieve therapeutic benefit. This is particularly crucial in the case of *trans*-splicing approaches for dominant mutations where the vast majority of deleterious mRNAs must be converted into normal transcripts. Intriguingly, *trans*-splicing was more efficient *in vitro* than *in vivo*, while PTMs expression was higher *in vivo* when produced from an AAV vector (4–7-folds). This phenomenon is likely due to the fact that the minigene reporter transcript used in *in vitro* experiments was more accessible to PTMs than the endogenous dystrophin pre-mRNA.

DMD patients with mutations in the 3′ part of the dystrophin gene (downstream of exon 59) are usually not eligible for dystrophin rescue by using exon skipping because this part of the gene encodes domains that are essential for dystrophin function. To address this point, we designed PTMs made of an AS annealing intron 58, and a cDNA comprising exons 59 to 79, which would be suitable to ~10% of the DMD population, whatever the nature of each patient mutation within this segment. Another advantage would be that such repair would provide a full-length protein with all its functional domains, something that cannot be achieved by using exon skipping. However, one must keep in mind that preexisting immunity against dystrophin has been noticed in some DMD patients, so immune response against full-length dystrophin might preclude dystrophin rescue strategies (51). Additionally, there is another issue that is often hidden: the PTM itself can be translated (Supplementary Figure S3B), even in the absence of a consensual Kozak sequence, giving rise to a truncated protein that can act either as an immunogenic trigger or as a dominant negative variant.

SUPPLEMENTARY DATA

Supplementary data are available at NAR Online, including Supplementary Reference [52].

ACKNOWLEDGEMENT

We are grateful to George Dickson for supplying the murine optimized microdystrophin plasmid, Vincent Mouly (Human Cell Culture Platform of the Myology Institute, Paris, France) for access to human immortalized DMD myoblasts, France Piétri-Rouxel for technical advice, the imagery platform 'Plate-forme d'Imagerie Cellulaire Pitié Salpêtrière', Etienne Mouisel and Christel Gentil for technical support and William Duddy for critical reading of the manuscript.

FUNDING

Association Française contre les Myopathies and Duchenne Parent Project Belgium/Netherlands. Funding for open access charge: Duchenne Parent Project Belgium/Netherlands.

Conflict of interest statement. None declared.

REFERENCES

1. Pramono,Z.A., Takeshima,Y., Alimsardjono,H., Ishii,A., Takeda,S. and Matsuo,M. (1996) Induction of exon skipping of the dystrophin transcript in lymphoblastoid cells by transfecting an antisense oligodeoxynucleotide complementary to an exon recognition sequence. *Biochem. Biophys. Res. Commun.*, **226**, 445–449.
2. Wilton,S.D., Lloyd,F., Carville,K., Fletcher,S., Honeyman,K., Agrawal,S. and Kole,R. (1999) Specific removal of the nonsense mutation from the mdx dystrophin mRNA using antisense oligonucleotides. *Neuromuscul. Disord.*, **9**, 330–338.
3. van Deutekom,J.C., Janson,A.A., Ginjaar,I.B., Frankhuizen,W.S., Aartsma-Rus,A., Bremmer-Bout,M., den Dunnen,J.T., Koop,K., van der Kooi,A.J., Goemans,N.M. *et al.* (2007) Local dystrophin restoration with antisense oligonucleotide PRO051. *N. Engl. J. Med.*, **357**, 2677–2686.
4. Kinali,M., Arechavala-Gomeza,V., Feng,L., Cirak,S., Hunt,D., Adkin,C., Guglieri,M., Ashton,E., Abbs,S., Nihoyannopoulos,P. *et al.* (2009) Local restoration of dystrophin expression with the morpholino oligomer AVI-4658 in Duchenne muscular dystrophy: a single-blind, placebo-controlled, dose-escalation, proof-of-concept study. *Lancet Neurol.*, **8**, 918–928.
5. Goemans,N.M., Tulinius,M., van den Akker,J.T., Burm,B.E., Ekhart,P.F., Heuvelmans,N., Holling,T., Janson,A.A., Platenburg,G.J., Sipkens,J.A. *et al.* (2011) Systemic administration of PRO051 in Duchenne's muscular dystrophy. *N. Engl. J. Med.*, **364**, 1513–1522.
6. Cirak,S., Arechavala-Gomeza,V., Guglieri,M., Feng,L., Torelli,S., Anthony,K., Abbs,S., Garralda,M.E., Bourke,J., Wells,D.J. *et al.* (2011) Exon skipping and dystrophin restoration in patients with Duchenne muscular dystrophy after systemic phosphorodiamidate morpholino oligomer treatment: an open-label, phase 2, dose-escalation study. *Lancet*, **378**, 595–605.
7. Michienzi,A., Prislei,S. and Bozzoni,I. (1996) U1 small nuclear RNA chimeric ribozymes with substrate specificity for the Rev pre-mRNA of human immunodeficiency virus. *Proc. Natl Acad. Sci. USA*, **93**, 7219–7224.
8. Gorman,L., Suter,D., Emerick,V., Schumperli,D. and Kole,R. (1998) Stable alteration of pre-mRNA splicing patterns by modified U7 small nuclear RNAs. *Proc. Natl Acad. Sci. USA*, **95**, 4929–4934.

9. Brun,C., Suter,D., Pauli,C., Dunant,P., Lochmuller,H., Burgunder,J.M., Schumperli,D. and Weis,J. (2003) U7 snRNAs induce correction of mutated dystrophin pre-mRNA by exon skipping. *Cell Mol. Life Sci.*, **60**, 557–566.
10. Goyenvalle,A., Vulin,A., Fougerousse,F., Leturcq,F., Kaplan,J.C., Garcia,L. and Danos,O. (2004) Rescue of dystrophic muscle through U7 snRNA-mediated exon skipping. *Science*, **306**, 1796–1799.
11. Denti,M.A., Rosa,A., D'Antona,G., Sthandier,O., De Angelis,F.G., Nicoletti,C., Allocca,M., Pansarasa,O., Parente,V., Musaro,A. *et al.* (2006) Chimeric adeno-associated virus/antisense U1 small nuclear RNA effectively rescues dystrophin synthesis and muscle function by local treatment of mdx mice. *Hum. Gene Ther.*, **17**, 565–574.
12. Benchaouir,R., Meregalli,M., Farini,A., D'Antona,G., Belicchi,M., Goyenvalle,A., Battistelli,M., Bresolin,N., Bottinelli,R., Garcia,L. *et al.* (2007) Restoration of human dystrophin following transplantation of exon-skipping-engineered DMD patient stem cells into dystrophic mice. *Cell Stem Cell*, **1**, 646–657.
13. Vulin,A., Barthelemy,I., Goyenvalle,A., Thibaud,J.L., Beley,C., Griffith,G., Benchaouir,R., Le Hir,M., Unterfinger,Y., Lorain,S. *et al.* (2012) Muscle function recovery in golden retriever muscular dystrophy after AAV1-U7 exon skipping. *Mol. Ther.*, **20**, 2120–2133.
14. Bish,L.T., Sleeper,M.M., Forbes,S.C., Wang,B., Reynolds,C., Singletary,G.E., Trafny,D., Morine,K.J., Sanmiguel,J., Cecchini,S. *et al.* (2012) Long-term restoration of cardiac dystrophin expression in golden retriever muscular dystrophy following rAAV6-mediated exon skipping. *Mol. Ther.*, **20**, 580–589.
15. Barbash,I.M., Cecchini,S., Faranesh,A.Z., Virag,T., Li,L., Yang,Y., Hoyt,R.F., Kornegay,J.N., Bogan,J.R., Garcia,L. *et al.* (2013) MRI roadmap-guided transendocardial delivery of exon-skipping recombinant adeno-associated virus restores dystrophin expression in a canine model of Duchenne muscular dystrophy. *Gene Ther.*, **20**, 274–282.
16. Harper,S.Q., Hauser,M.A., DelloRusso,C., Duan,D., Crawford,R.W., Phelps,S.F., Harper,H.A., Robinson,A.S., Engelhardt,J.F., Brooks,S.V. *et al.* (2002) Modular flexibility of dystrophin: implications for gene therapy of Duchenne muscular dystrophy. *Nat. Med.*, **8**, 253–261.
17. Aartsma-Rus,A., Fokkema,I., Verschuuren,J., Ginjaar,I., van,D.J., van Ommen,G.J. and den Dunnen,J.T. (2009) Theoretic applicability of antisense-mediated exon skipping for Duchenne muscular dystrophy mutations. *Hum. Mutat.*, **30**, 293–299.
18. Horiuchi,T. and Aigaki,T. (2006) Alternative trans-splicing: a novel mode of pre-mRNA processing. *Biol. Cell*, **98**, 135–140.
19. Gingeras,T.R. (2009) Implications of chimaeric non-co-linear transcripts. *Nature*, **461**, 206–211.
20. Puttaraju,M., Jamison,S.F., Mansfield,S.G., Garcia-Blanco,M.A. and Mitchell,L.G. (1999) Spliceosome-mediated RNA trans-splicing as a tool for gene therapy. *Nat. Biotechnol.*, **17**, 246–252.
21. Chao,H., Mansfield,S.G., Bartel,R.C., Hiriyanna,S., Mitchell,L.G., Garcia-Blanco,M.A. and Walsh,C.E. (2003) Phenotype correction of hemophilia A mice by spliceosome-mediated RNA trans-splicing. *Nat. Med.*, **9**, 1015–1019.
22. Coady,T.H., Baughan,T.D., Shababi,M., Passini,M.A. and Lorson,C.L. (2008) Development of a single vector system that enhances trans-splicing of SMN2 transcripts. *PLoS. One.*, **3**, e3468.
23. Tahara,M., Pergolizzi,R.G., Kobayashi,H., Krause,A., Luettich,K., Lesser,M.L. and Crystal,R.G. (2004) Trans-splicing repair of CD40 ligand deficiency results in naturally regulated correction of a mouse model of hyper-IgM X-linked immunodeficiency. *Nat. Med.*, **10**, 835–841.
24. Liu,X., Luo,M., Zhang,L.N., Yan,Z., Zak,R., Ding,W., Mansfield,S.G., Mitchell,L.G. and Engelhardt,J.F. (2005) Spliceosome-mediated RNA trans-splicing with recombinant adeno-associated virus partially restores cystic fibrosis transmembrane conductance regulator function to polarized human cystic fibrosis airway epithelial cells. *Hum. Gene Ther.*, **16**, 1116–1123.
25. Mansfield,S.G., Clark,R.H., Puttaraju,M., Kole,J., Cohn,J.A., Mitchell,L.G. and Garcia-Blanco,M.A. (2003) 5' exon replacement and repair by spliceosome-mediated RNA trans-splicing. *RNA*, **9**, 1290–1297.
26. Lorain,S., Peccate,C., Le Hir,M. and Garcia,L. (2010) Exon exchange approach to repair Duchenne dystrophin transcripts. *PLoS One*, **5**, e10894.
27. Koller,U., Wally,V., Mitchell,L.G., Klausegger,A., Murauer,E.M., Mayr,E., Gruber,C., Hainzl,S., Hintner,H. and Bauer,J.W. (2011) A novel screening system improves genetic correction by internal exon replacement. *Nucleic Acids Res.*, **39**, e108.
28. Foster,H., Sharp,P.S., Athanasopoulos,T., Trollet,C., Graham,I.R., Foster,K., Wells,D.J. and Dickson,G. (2008) Codon and mRNA sequence optimization of microdystrophin transgenes improves expression and physiological outcome in dystrophic mdx mice following AAV2/8 gene transfer. *Mol. Ther.*, **16**, 1825–1832.
29. Zufferey,R., Nagy,D., Mandel,R.J., Naldini,L. and Trono,D. (1997) Multiply attenuated lentiviral vector achieves efficient gene delivery *in vivo*. *Nat. Biotechnol.*, **15**, 871–875.
30. Lorain,S., Gross,D.A., Goyenvalle,A., Danos,O., Davoust,J. and Garcia,L. (2008) Transient immunomodulation allows repeated injections of AAV1 and correction of muscular dystrophy in multiple muscles. *Mol. Ther.*, **16**, 541–547.
31. Le Guiner,C., Moullier,P. and Arruda,V.R. (2011) Biodistribution and shedding of AAV vectors. *Methods Mol. Biol.*, **807**, 339–359.
32. Charrier,S., Stockholm,D., Seye,K., Opolon,P., Taveau,M., Gross,D.A., Bucher-Laurent,S., Delenda,C., Vainchenker,W., Danos,O. *et al.* (2005) A lentiviral vector encoding the human Wiskott-Aldrich syndrome protein corrects immune and cytoskeletal defects in WASP knockout mice. *Gene Ther.*, **12**, 597–606.
33. Decary,S., Mouly,V., Hamida,C.B., Sautet,A., Barbet,J.P. and Butler-Browne,G.S. (1997) Replicative potential and telomere length in human skeletal muscle: implications for satellite cell-mediated gene therapy. *Hum. Gene Ther.*, **8**, 1429–1438.
34. Mamchaoui,K., Trollet,C., Bigot,A., Negroni,E., Chaouch,S., Wolff,A., Kandalla,P.K., Marie,S., Di,S.J., St Guily,J.L. *et al.* (2011) Immortalized pathological human myoblasts: towards a universal tool for the study of neuromuscular disorders. *Skelet. Muscle*, **1**, 34.
35. Amalfitano,A. and Chamberlain,J.S. (1996) The mdx-amplification-resistant mutation system assay, a simple and rapid polymerase chain reaction-based detection of the mdx allele. *Muscle Nerve*, **19**, 1549–1553.
36. Morris,G., Man,N. and Sewry,C.A. (2011) Monitoring duchenne muscular dystrophy gene therapy with epitope-specific monoclonal antibodies. *Methods Mol. Biol.*, **709**, 39–61.
37. Sicinski,P., Geng,Y., Ryder-Cook,A.S., Barnard,E.A., Darlison,M.G. and Barnard,P.J. (1989) The molecular basis of muscular dystrophy in the mdx mouse: a point mutation. *Science*, **244**, 1578–1580.
38. Gregorevic,P., Allen,J.M., Minami,E., Blankinship,M.J., Haraguchi,M., Meuse,L., Finn,E., Adams,M.E., Froehner,S.C., Murry,C.E. *et al.* (2006) rAAV6-microdystrophin preserves muscle function and extends lifespan in severely dystrophic mice. *Nat. Med.*, **12**, 787–789.
39. Black,D.L. (1991) Does steric interference between splice sites block the splicing of a short c-src neuron-specific exon in non-neuronal cells? *Genes Dev.*, **5**, 389–402.
40. Wang,J., Mansfield,S.G., Cote,C.A., Jiang,P.D., Weng,K., Amar,M.J., Brewer,B.H. Jr, Remaley,A.T., McGarrity,G.J., Garcia-Blanco,M.A. *et al.* (2009) Trans-splicing into highly abundant albumin transcripts for production of therapeutic proteins *in vivo*. *Mol. Ther.*, **17**, 343–351.
41. Yeo,G. and Burge,C.B. (2004) Maximum entropy modeling of short sequence motifs with applications to RNA splicing signals. *J. Comput. Biol.*, **11**, 377–394.
42. Chapman,V.M., Miller,D.R., Armstrong,D. and Caskey,C.T. (1989) Recovery of induced mutations for X chromosome-linked muscular dystrophy in mice. *Proc. Natl Acad. Sci. USA*, **86**, 1292–1296.
43. Smith,P.J., Zhang,C., Wang,J., Chew,S.L., Zhang,M.Q. and Krainer,A.R. (2006) An increased specificity score matrix for the prediction of SF2/ASF-specific exonic splicing enhancers. *Hum. Mol. Genet.*, **15**, 2490–2508.

44. Cartegni,L., Wang,J., Zhu,Z., Zhang,M.Q. and Krainer,A.R. (2003) ESEfinder: a web resource to identify exonic splicing enhancers. *Nucleic Acids Res.*, **31**, 3568–3571.
45. Lu,Q.L., Mann,C.J., Lou,F., Bou-Gharios,G., Morris,G.E., Xue,S.A., Fletcher,S., Partridge,T.A. and Wilton,S.D. (2003) Functional amounts of dystrophin produced by skipping the mutated exon in the mdx dystrophic mouse. *Nat. Med.*, **9**, 1009–1014.
46. Buvoli,M., Buvoli,A. and Leinwand,L.A. (2007) Interplay between exonic splicing enhancers, mRNA processing, and mRNA surveillance in the dystrophic Mdx mouse. *PLoS One*, **2**, e427.
47. Palmiter,R.D., Sandgren,E.P., Avarbock,M.R., Allen,D.D. and Brinster,R.L. (1991) Heterologous introns can enhance expression of transgenes in mice. *Proc. Natl Acad. Sci. USA*, **88**, 478–482.
48. Lu,S. and Cullen,B.R. (2003) Analysis of the stimulatory effect of splicing on mRNA production and utilization in mammalian cells. *RNA.*, **9**, 618–630.
49. Nott,A., Meislin,S.H. and Moore,M.J. (2003) A quantitative analysis of intron effects on mammalian gene expression. *RNA*, **9**, 607–617.
50. Liu,X., Jiang,Q., Mansfield,S.G., Puttaraju,M., Zhang,Y., Zhou,W., Cohn,J.A., Garcia-Blanco,M.A., Mitchell,L.G. and Engelhardt,J.F. (2002) Partial correction of endogenous DeltaF508 CFTR in human cystic fibrosis airway epithelia by spliceosome-mediated RNA trans-splicing. *Nat. Biotechnol.*, **20**, 47–52.
51. Mendell,J.R., Campbell,K., Rodino-Klapac,L., Sahenk,Z., Shilling,C., Lewis,S., Bowles,D., Gray,S., Li,C., Galloway,G. *et al.* (2010) Dystrophin immunity in Duchenne's muscular dystrophy. *N. Engl. J. Med.*, **363**, 1429–1437.
52. Bartoli,M., Poupiot,J., Goyenvalle,A., Perez,N., Garcia,L., Danos,O. and Richard,I. (2006) Noninvasive monitoring of therapeutic gene transfer in animal models of muscular dystrophies. *Gene Ther.*, **13**, 20–28.